Active-site-mutagenesis study of rat liver betaine–homocysteine S-methyltransferase

Beatriz GONZÁLEZ*, Nuria CAMPILLO†, Francisco GARRIDO‡, María GASSET*, Juliana SANZ-APARICIO* and María A. PAJARES‡[1]

*Instituto de Química-Física 'Rocasolano' (CSIC), Serrano 119, 28006 Madrid, Spain, †Instituto de Química Médica (CSIC), Juan de la Cierva 3, 28006 Madrid, Spain, and ‡Instituto de Investigaciones Biomédicas 'Alberto Sols' (CSIC-UAM), Arturo Duperier 4, 28029 Madrid, Spain

A site-directed-mutagenesis study of putative active-site residues in rat liver betaine–homocysteine S-methyltransferase has been carried out. Identification of these amino acids was based on data derived from a structural model of the enzyme. No alterations in the CD spectra or the gel-filtration chromatography elution pattern were observed with the mutants, thus suggesting no modification in the secondary structure content or in the association state of the proteins. All the mutants obtained showed a reduction of the enzyme activity, the most dramatic effect being that of Glu^{159}, followed by Tyr^{77} and Asp^{26}. Changes in affinity for either of the substrates, homocysteine or betaine, were detected when substitutions were performed of Glu^{21}, Asp^{26}, Phe^{74} and Cys^{186}. Interestingly, Asp^{26}, postulated to be involved in homocysteine binding, has a strong effect on affinity for betaine. The relevance of these results is discussed in the light of very recent structural data obtained for the human enzyme.

Key words: homocysteine metabolism, kinetic study, methionine metabolism, site-directed mutagenesis, structural modelling.

INTRODUCTION

Homocysteine (Hcy) represents a key branchpoint in methionine metabolism [1]. Its synthesis is catalysed by *S*-adenosylhomocysteine (AdoHcy) hydrolase (EC 3.3.1.1) in a reaction that is thermodynamically shifted to the production of AdoHcy. This compound is a potent inhibitor of the transmethylation reactions dependent on *S*-adenosylmethionine (AdoMet) [2] and, therefore, elimination of Hcy has to be carried out, coupled with its synthesis, to maintain the methylation ratio AdoMet/AdoHcy. The three enzymes that use Hcy are cystathionine β-synthase (CBS; EC 4.2.1.22), methionine synthase (EC 2.1.1.13) and betaine–homocysteine S-methyltransferase (BHMT; EC 2.1.1.5). CBS initiates the *trans*-sulphuration pathway leading to cystathionine, which is further used for the synthesis of cysteine [3]. The other two enzymes remethylate Hcy to render methionine in reactions that use different methyl donors, methyltetrahydrofolate and betaine. These methyl donors connect the pathway with folate metabolism and choline oxidation, allowing the recovery of one of the methylation equivalents used in choline synthesis, leading to the incorporation of four of its carbon units into the one-carbon pool [1]. This picture is completed by the fact that AdoMet, vitamin B_6 and vitamin B_{12} control, directly or indirectly, the activity of these three enzymes. Alterations in the Hcy levels reflect changes in any of the reactions mentioned above. Thus homocystinuria has been related to deficiencies in CBS and methylene tetrahydrofolate reductase (EC 1.7.99.5). Moreover, increased plasma levels of Hcy (hyperhomocysteinaemia) have also been detected in patients with cardiovascular disease, and this increase is thus considered an independent risk factor for the development of this type of illness [4,5].

BHMT is the least studied enzyme of Hcy metabolism. Most of these enzymes are oligomers, composed of four identical subunits [6–8], and the one in rat liver contains 407 amino acids (accession no. AF038870). Its localization is cytosolic and is restricted to the liver and kidney in most of the species studied [9,10], but its appearance in lens has also been reported in Rhesus monkeys [11]. Conservation among mammalian enzymes is very high, being more than 80% identical at the nucleotide level and more than 90% at the amino acid level for the rat, human, mouse and pig liver proteins [12]. This enzyme contains zinc coordinated to three conserved cysteine residues (positions 217, 299 and 300 according to the human sequence) [13,14]. One of the mutations detected so far in patients with moderate hyperhomocysteinaemia (G199S, $Gly^{199} \rightarrow Ser$) has been suggested to play an important role in the secondary structure (SS) of the enzyme [15]. Alterations of betaine levels and decreases in BHMT activity have been observed in choline deficiencies [16], whereas in methionine deficiencies the enzyme maintains the levels of this essential amino acid for mammalian growth and development [17]. In vitamin B_{12}-deficient diets, a decrease in enzyme activity has been observed [18], whereas increases have been detected in animals given low-protein diets combined with alcohol, alcohol liquid diets, high-protein diets or methionine-supplemented diets [19]. Studies in developing rats have shown that liver activity in the foetus is lower than that in the adult, a peak being observed in the first 10 days in the newborn [20]. Expression of BHMT mRNA is decreased in cirrhotic livers and hepatocellular carcinoma [21,22] and is increased in tissue samples from animals on a methionine-deficient diet [23]. Moreover, cortisol and thyroxine treatments also affect BHMT activity [20]. Previously, it has been shown that BHMT regulates the expression of apolipoprotein B, leading to an increase in related lipoproteins [12], and it has been located bound to tubulin in liver extracts [24]. On the other hand, betaine has been proposed to play a role in the protection of proteins against denaturation in kidney, due to the high level of urea accumulated in the cells [25], a similar role being ascribed to the lens BHMT [11].

Finally, structural data on this enzyme are very limited and, hence, the objective of the present study is to get an insight into the role of active-site residues. For this purpose, we have built a

Abbreviations used: ADA, adenosine deaminase; AdoHcy, *S*-adenosylhomocysteine; AdoMet, *S*-adenosylmethionine; BHMT, betaine–homocysteine S-methyltransferase; CB-Hcy, *S*-(δ-carboxybutyl)-L-homocysteine; CBS, cystathionine β-synthase; E21K, $Glu^{21} \rightarrow Lys$ mutation; Hcy, homocysteine; SS, secondary structure.

[1] To whom correspondence should be addressed (e-mail mapajares@iib.uam.es).

structural model of the rat liver protein and the role of the proposed active-site amino acids has been tested by site-directed mutagenesis. The validity of the identification of catalytically important residues derived from this model has been confirmed with the report of the first structure of a human BHMT complex [8] while the present manuscript was in preparation. Therefore our results are discussed in the light of the data derived from that X-ray structure.

EXPERIMENTAL

Materials

Betaine, Hcy thiolactone, PMSF, pepstatin A, aprotinin, leupeptin, antipain, dithiothreitol, ampicillin, Freund's adjuvant and the molecular-mass standards for gel-filtration chromatography were obtained from Sigma (St. Louis, MO, U.S.A.). [methyl-^{14}C]Choline chloride (50–60 mCi/mmol) was supplied by Amersham International (Little Chalfont, Bucks., U.K.). Isopropyl β-D-thiogalactoside was obtained from AMBION (Austin, TX, U.S.A.). Superose 12 HR 10/30 was purchased from Amersham Pharmacia (Uppsala, Sweden). Optiphase HiSafe 3 scintillation fluid was obtained from E&G Wallac (Milton Keynes, U.K.). Goat anti-rabbit IgG–horseradish peroxidase, Bio-Rad protein assay kit I and the electrophoresis reagents were obtained from Bio-Rad Laboratories (Richmond, CA, U.S.A.). YM-30 ultrafiltration membranes were purchased from AMICON Corp. (Beverly, MA, U.S.A.). Chemiluminescence Renaissance reagents were obtained from DuPont New England Nuclear (Boston, MA, U.S.A.). Triton X-100 was purchased from Merck (Darmstadt, Germany). QuikChange site-directed mutagenesis kit and the Impact-CN system were supplied by Stratagene (La Jolla, CA, U.S.A.) and New England Biolabs (Beverly, MA, U.S.A.) respectively. The rest of the buffers and reagents were of the best quality commercially available.

Sequence alignments, SS prediction and template searching

The sequence of rat liver BHMT (SwissProt O09171) was used to search for similar enzymes and to predict the SS. Homologous proteins have been searched using Psi-BLAST server [26]. Alignments between BHMT and other enzyme sequences were made with the CLUSTAL X program [27] and were corrected manually when necessary. For SS prediction, three different methods were used: PHD [28], PSIPRED [29] and JPRED [30]. We considered secondary elements with a score over six as reliable (nine being the maximum). All these three methods provided very similar results.

On initiating the present study, no structure for the BHMT family of enzymes was available, as revealed by a Psi-BLAST search. Thus, to find a template for BHMT model building, different strategies were tried. First, some enzymes with a known structure and functionally related to BHMT, such as Zn^{2+}-dependent transferases or methyltransferases, were tested as possible templates, with no success. Therefore protein-fold recognition methods were applied using 3D-PSSM [31], THREADER [32] and BIOINBGU [33] threading algorithms. Enzymes with good scores by at least two methods were tested as templates for BHMT homology modelling, and were used to build a preliminary model when the following criteria were fulfilled: (1) their SS correlated with BHMT SS prediction, and (2) some relevant residue conservation was observed.

Homology modelling of the BHMT protein structure

A three-dimensional structure for BHMT has been modelled by comparative protein modelling methods using the MODELLER package [34]. This program uses spatial restraints from the input templates and the model to be built has to satisfy the restraints as much as possible. Preliminary models were built from an alignment based on SS correlation between the templates and the predicted BHMT SS. To consider definitively a protein as a good template, the cysteines involved in Zn^{2+} binding had to be orientated properly in the preliminary models. One of the proteins tested, adenosine deaminase (ADA), fulfilled all the selection criteria and, hence, was used as a template (pdb code: 1a4l) [35]. Initially, 15 BHMT models were built, but only the one with the least restraints violation and the lowest energy was evaluated, and several cycles of realignment and model building were repeated until no further optimization of the model was obtained. The final model was evaluated with VERIFY3D [36] and PROCHECK [37]. JOY [38] and COMPARER [39] programs were used to generate structure-based alignments between the target and the template in every cycle of the model-building process.

Expression of the fusion protein and purification of rat liver BHMT

The sequence of rat liver BHMT included in the *Nde*I–*Bam*HI sites of the pET11a expression vector [7] was cloned in pBluescript M13 (+) KS, and later in the *Nde*I–*Not*I restriction sites of pTYB12, to obtain an intein–chitin-binding BHMT fusion protein. Competent *Escherichia coli* BL21(DE3) cells were transformed with the plasmid pBHMT-TYB12, and 1 litre of cultures was grown in Luria–Bertani medium containing 100 μg/ml ampicillin. Induction was performed for 16 h at 20 °C by adding 0.5 mM isopropyl β-D-thiogalactoside at A_{595} 0.6. Cells were harvested by centrifugation, washed with water and stored at −70 °C until use. Disruption of the cell pellets was performed by sonication at 4 °C in a Branson 250 sonifier (30 pulses of 30 s at 30 s intervals, output power level 20) in 10 vol of 20 mM Tris/HCl (pH 8.0) containing 0.5 M NaCl, 0.1 mM EDTA, 0.1 % (v/v) Triton X-100 and protease inhibitors (2 μg/ml aprotinin, 1 μg/ml pepstatin A, 0.5 μg/ml leupeptin, 2.5 μg/ml antipain, 0.1 mM benzamidine and 0.1 mM PMSF). The soluble fraction was separated by centrifugation for 30 min at 13000 ***g*** and loaded on Chitin beads (10 ml) for purification. The column was washed first with 30 bed volumes of the buffer, followed by 10 vol of 20 mM Tris/HCl (pH 8.0), containing 50 mM NaCl, 0.1 mM EDTA (buffer A) and 3 vol of buffer A containing 30 mM 2-mercaptoethanol (buffer B). The column was incubated for 48 h at room temperature (23 °C) to allow intein cleavage and eluted with 3 vol of buffer B. The purified preparation was then dialysed against buffer A (3 litres) to eliminate a small peptide that originated during cleavage of the fusion protein. The final purification yield was 4 mg/g of bacteria. For storage, purified BHMT was added to 50 % glycerol and kept at −20 °C.

Site-directed mutagenesis

Residues of interest were mutated using the QuikChange site-directed mutagenesis method, following the manufacturer's instructions. Mutants were constructed in the vector pBHMT-TYB12 using the mutagenic oligonucleotides included in Table 1. Mutations were verified by sequencing the entire cDNA, using the dideoxy termination method [40].

Activity and kinetic determinations

BHMT activity was determined for 1 h at 37 °C using the radioassay described previously [3]. Kinetics for Hcy and betaine

Table 1 Mutagenic oligonucleotides

The primers synthesized for site-directed mutagenesis are included. Only the sense strand is shown, and the substitution performed appears underlined.

Mutant	Mutagenic oligonucleotide
E21A	5′-GCTTAAATGCTGGCGCAGTCGTGATCGG-3′
E21K	5′-CGCTTAAATGCTGGCAAAGTCGTGATCGG-3′
D26A	5′-GTCGTGATCGGAGCTGGGGGATTTGTC-3′
D26I	5′-GTCGTGATCGGAATTGGGGGATTTGTC-3′
T73G	5′-CGAACGTCATGCAGGGCTTCACTTTCTATGC-3′
F74A	5′-CGAACGTCATGCAGACCGCCACTTTCTATGC-3′
Y77A	5′-GCAGACCTTCACTTTCGCTGCAAGTGAGGAC-3′
A119G	5′-GGATGCATTGGTTGGAGGAGGTGTGAG-3′
E159G	5′-GGACTTCCTCATTGCAGGGTATTTTGAACATG-3′
E159K	5′-GGACTTCCTCATTGCAAAGTATTTTGAACATG-3′
T184G	5′-GCCTATAGCGGCTGGCATGTGCATCGG-3′
C186S	5′-GCGGCTACCATGTCCATCGGACCTG-3′
C186A	5′-GCGGCTACCATGGCCATCGGACCTG-3′

were performed in a concentration range between 1 μM and 6.5 mM at a saturating concentration of either 6.5 mM betaine or 6.5 mM Hcy.

Determination of SS

Far-UV CD spectra of purified BHMT and mutants were recorded on a Jasco J-810 spectropolarimeter at 25 °C [41], using samples of 0.1–0.2 mg/ml protein concentration and 0.1 cm pathlength cuvettes. After baseline subtraction, the observed ellipticities were converted into mean residue ellipticities (θ_{mrw}) on the basis of a mean molecular mass/residue of 0.110 kDa. SS composition was calculated using the Jasco software. A minimum of five spectra were taken for each sample.

Gel-filtration chromatography

Samples of wild-type and mutant BHMT of 100 μl (50 μg) were injected on a Superose 12 HR 10/30 gel-filtration column connected to an Advanced Protein Purification System (Waters, Millipore Corp., Milford, MA, U.S.A.). Equilibration and elution were performed using 20 mM Tris/HCl (pH 8.0) containing 200 mM NaCl and 0.1 mM EDTA at a flow rate of 0.3 ml/min at 4 °C. Absorbance at 280 nm was recorded and 210 μl fractions were collected to detect the presence of BHMT by dot-blot. The protein standards used and their elution volumes were as follows: Dextran Blue (2000 kDa), 8.69 ml; apoferritin (443 kDa), 9.87 ml; β-amylase (200 kDa), 11.34 ml; alcohol dehydrogenase (150 kDa), 12.07 ml; carbonic anhydrase (29 kDa), 15.12 ml; and ATP (0.551 kDa), 19.26 ml.

Production of a polyclonal anti-BHMT antiserum

Rat liver BHMT purified as described by González et al. [7] was used to immunize New Zealand rabbits. Preimmune serum was obtained before injection of the antigen. The immunization method used was the same as that described previously by our laboratory [42]. The specificity of the response was tested by immunoblotting (Figure 1), and the best results were obtained using a 1:50000 dilution (v/v) of the antiserum.

SDS/PAGE and Western blotting

Denaturing gel electrophoresis of the samples was performed by SDS/PAGE (10 % gel). Staining was performed using Coomassie Blue R-250. When needed, a Western blot of the gel was performed using the buffer system described by Mingorance et al. [42], and revealed using the anti-BHMT antiserum mentioned above.

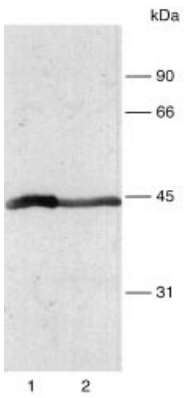

Figure 1 Specificity of the anti-BHMT antiserum

BHMT was purified and used for rabbit immunization as described in the Experimental section. Immune serum was collected and used to test for specificity in Western blot. For this purpose, 10 μg of either purified protein (lane 1) or rat liver cytosol (lane 2) was loaded on SDS/PAGE gels and transferred to nitrocellulose membranes. The molecular mass of the markers is given on the right-hand side.

Dot-blot

Samples of the column fractions (maximum volume 50 μl) were spotted on nitrocellulose membranes. After denaturation using 6 M guanidinium chloride (50 μl), the membrane was washed twice with TTBS, before the blocking step using low-fat dry milk (3 %, w/v). The membrane was washed again with TTBS and incubated with a 1:50000 (v/v) solution of the anti-BHMT polyclonal antiserum prepared in our laboratory. Under these conditions, the only band detected corresponds to BHMT, as judged by SDS/PAGE gels (Figure 1). Membranes were revealed using Renaissance, the exposed films were subjected to densitometric scanning and the data were used to elaborate the elution profile.

Determination of the protein concentration

The protein concentration of the samples was measured either by using the Bio-Rad kit I, with BSA as a standard, or spectrophotometrically using a calculated molar absorbance coefficient ϵ at 280 nm of 58020 $M^{-1} \cdot cm^{-1}$ in 6 M guanidinium chloride. This coefficient calculated from the sequence was corrected appropriately for the mutants.

RESULTS AND DISCUSSION

BHMT belongs to the family of thiol/selenol methyltransferases. Sequence similarity among these enzymes is not high, but a strong conservation of two motifs, which include the three cysteine residues involved in zinc binding, is observed. In addition, SS prediction renders very similar results for all these proteins (Figure 2). Thus it is believed that all of them may share a common folding. At the start of the present study, no structure for this family of proteins was available, except for two domains

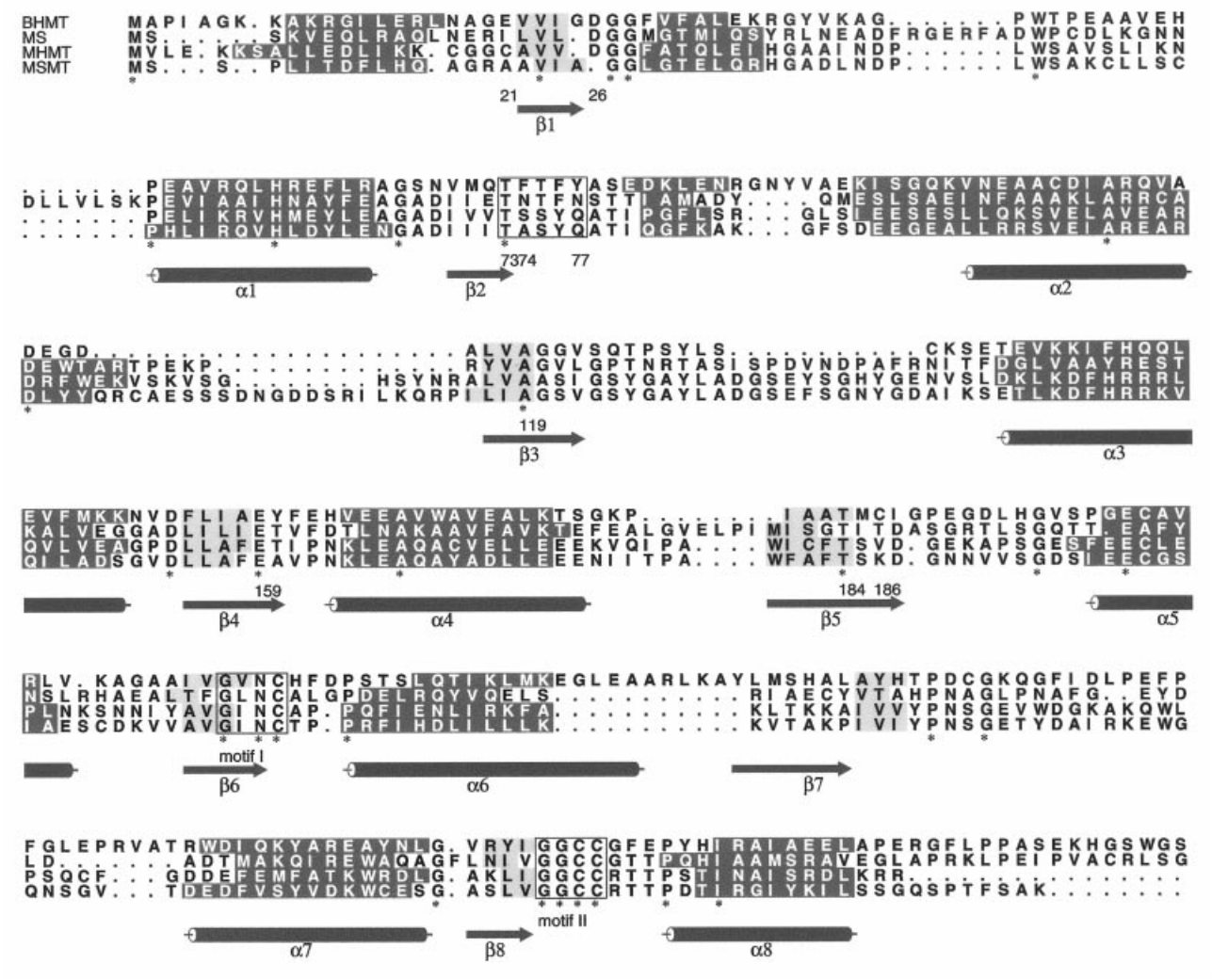

Figure 2 Alignment of enzyme sequences belonging to the thiol/selenol methyltransferase family

The alignment includes data from the thiol/selenol methyltransferase family. The highly conserved SS prediction among these proteins is presented as grey-shaded regions (α-helix with white characters and β-strands with black characters). The α-helices and β-strands comprising the barrel in the human BHMT crystal structure are highlighted below the sequences. As can be observed, only β2 was not predicted. The conserved residues are marked with an asterisk below the sequence alignment, whereas the residues mutated in the present study are indicated by their sequence number. Motifs I and II comprising the Zn^{2+}-binding residues (Cys^{217}, Cys^{299} and Cys^{300}) are boxed, as is the conserved motif TX(ST)(YF)X. Proteins aligned are as follows: rat liver BHMT, *E. coli* B_{12}-dependent methionine synthase (MS), *S*-methylmethionine homocysteine methyltransferase from *Arabidopsis thaliana* (MHMT) and *S*-methylmethionine selenocysteine methyltransferase from *Astralagus bisulcatus* (MSMT).

of the vitamin B_{12}-dependent methionine synthase that have no identity with BHMT [43,44]. Consequently, it was necessary to search for templates among possible structural homologues to build a model for the BHMT structure. Thus searches were performed based on either functional similarity or fold-recognition methods, success being achieved only by the use of the latter. Most of the suggested templates presented the typical TIM barrel fold, but only those proposed by at least two of the methods employed were used to build preliminary models. Further selection was made based on the following criteria: (i) good correlation between their SS and that predicted for BHMT, (ii) conservation of catalytically relevant residues in key areas of the protein and (iii) correct positioning of the cysteines involved in zinc binding according to the previous data for BHMT [14]. Only mouse ADA fulfilled these criteria and, hence, was considered for further analysis.

Mouse ADA belongs to the family of metal-dependent hydrolases and catalyses the hydrolysis of adenine to render inosine. This is a reaction linked to methionine metabolism, since, among other pathways, adenine can be produced by AdoHcy hydrolysis in the same reaction that leads to Hcy [45]. Moreover, ADA is a zinc-dependent metalloenzyme in which the metal assumes the same role postulated in BHMT, activating a water molecule for a further nucleophilic attack [35,46,47]. Sequence similarity between BHMT and ADA is 52%, with only 13% identity. Their predicted SS correlates well and, in addition, some of the zinc ligands are conserved (Cys^{217} of BHMT aligns with His^{214} of ADA, and both Cys^{299} and Cys^{300} of BHMT align with Asp^{297} of ADA) (Figure 3). The structural model constructed does not include the 47 N-terminal amino acids. This segment is absent from many of the members of the thiol/selenol family, suggesting a non-essential role of this area for the overall folding. The best

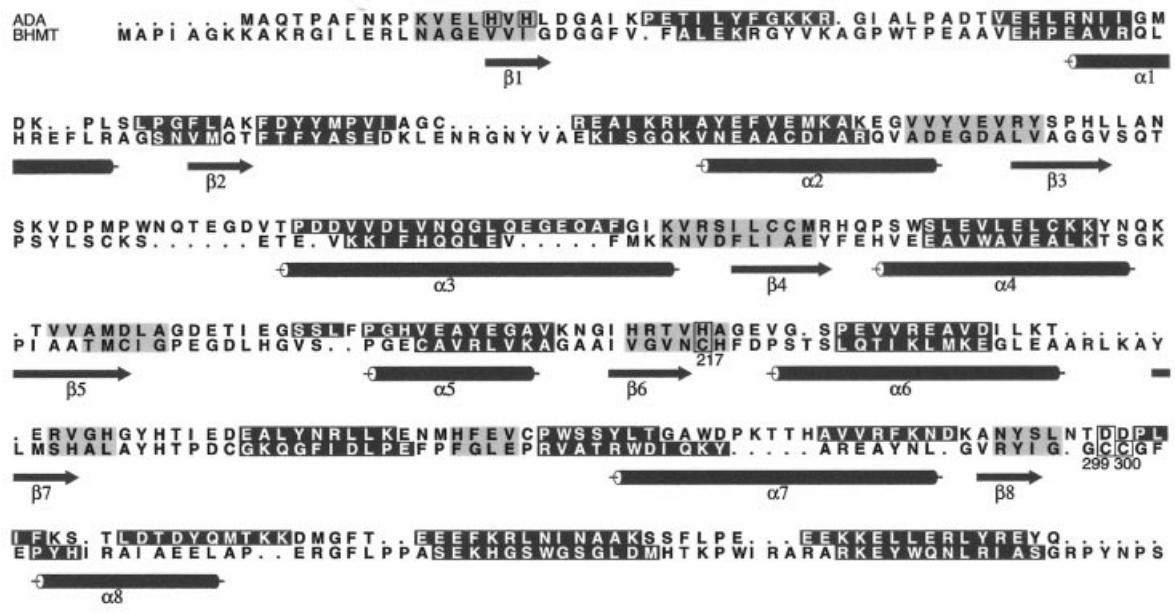

Figure 3 Alignment of mouse ADA and rat liver BHMT used in the construction of the model

SS elements, α-helices and β-strands (grey-shaded regions with white and black characters respectively) of ADA and those built for the BHMT model are shown. The SS elements comprising the barrel in the human BHMT crystal structure are represented schematically below the sequence alignment. As can be observed, 7 out of 8 β/α blocks were assigned properly in the BHMT model. Zn^{2+} ligands identified for both enzymes are boxed.

Figure 4 Structural model for rat liver BHMT

The structural model of BHMT built using mouse ADA as a template revealed an $(\alpha/\beta)_8$ barrel as the monomer fold. The main SS elements appear in grey (α-helices) and black (β-strands). The three cysteine residues involved in Zn^{2+} binding are represented as ball and sticks, and the zinc atom was modelled between them.

model obtained is shown in Figure 4. The proposed BHMT structure is an $(\alpha/\beta)_8$ barrel, in which the three cysteines identified as zinc ligands (Cys^{217}, Cys^{299} and Cys^{300}) are pointing to the centre of the barrel. One of the eight (α/β) blocks comprising the core of the barrel was not predicted for the thiol/selenol methyltransferases and was introduced into the model on the basis of the alignment with ADA. The final model presents only 2.6% of the residues located in disallowed regions according to a Ramachandran plot, which is an acceptable value for models constructed using this approach. Evaluation of the model with VERIFY3D program produces entirely positive scores.

The typical $(\alpha/\beta)_8$ barrel fold is one of the largest and most regular structures described to date. Several features are repeated in all the proteins folded this way, one of them being the location of the active site at the centre of the barrel's cavity. As shown in Figure 2, β-strands and α-helices are more conserved and form the barrel's core, whereas more variability is present in the loops. Residues involved in catalysis are located in the strands surrounding the cavity, and the loops following the C-terminal ends of these strands provide the amino acids related to substrate specificity. In our model, the highly conserved motifs I [G(LIV)NC^{217}] and II ($GGCC^{300}$) [14], containing the zinc-binding cysteines, are located in loops at the C-terminal ends of two β-strands in the barrel. Moreover, due to the fact that this family of enzymes binds zinc and uses Hcy, it is possible to postulate that the most conserved loops are related to their binding. Following the same criteria, those areas that are less preserved, but common among enzymes using the same methyl donor, could be related to betaine binding. Thus several interesting residues have been identified in our model: Glu^{21}, Asp^{26}, Thr^{73}, Phe^{74}, Tyr^{77}, Ala^{119}, Glu^{159}, Thr^{184} and Cys^{186}. Some of them have been selected due to their correct location at the C-terminal ends of β-strands in the model. Besides, they are conserved in all the enzymes of the family (Ala^{119}, Glu^{159} and Thr^{184}), align with relevant residues of ADA (Glu^{21} and Asp^{26}) or were proposed to be next to the Zn^{2+}-binding site (Cys^{186}) (Figure 3). The rest of the selected residues (Thr^{73}, Phe^{74} and Tyr^{77}) are present in a conserved motif, $T^{73}X(ST)(YF)$, which contains more aromatic amino acids directed to the barrel's

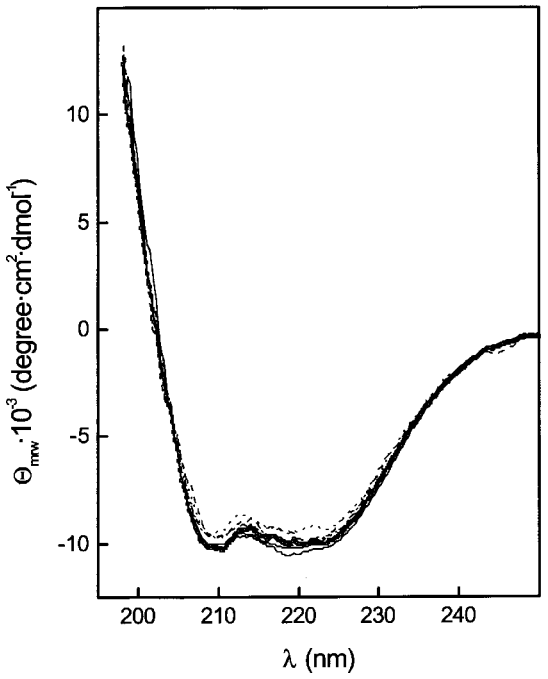

Figure 5 CD spectra of wild-type and mutant BHMT

Only CD spectra of wild-type and the most relevant mutants, whose activity is less than 15% of that of the wild-type, are shown for graphical purposes. ——, Wild-type; – – –, D26I; ....., Y77A; –□–, E159G; ——, E159K. Spectra are the averages of five scans.

Table 2 Comparison of the content of SS elements

Data for the content of the main SS elements obtained from CD spectra are compared with those derived from prediction methods and X-ray diffraction studies on human BHMT. CD calculation is within the 10% error due to protein concentration measurements. Predicted and X-ray diffraction values are based on 360 amino acids, which are those shown in the solved structure.

	CD spectra (%)	Predicted (%)	X-ray diffraction (%)
α-Helix	28.6	34	38
β-Sheet	31.4	7	11
Turns	10.1		20
Random coil	20.9		31

cavity, as required for betaine binding [48]. All these facts make these residues ideal candidates for further study using site-directed mutagenesis.

To establish clearly the role of the residues identified in the structural model, several mutants were prepared (Table 1). For this purpose, the IMPACT CN system was used, since it allowed a faster purification to homogeneity of the proteins under study. In our case, the expression vector of choice was pTYB12, to protect the BHMT N-terminus from bacterial aminopeptidases. Cleavage was achieved as described by Breksa and Garrow [14], leading to a BHMT protein having three extra amino acids, Ala, Gly and His, at its N-terminus. Addition of these extra residues did not interfere with either activity or SS, since the levels of methionine synthesis achieved and the CD spectra were similar to those obtained from a liver-purified BHMT (18.7 nmol · min^{-1} · mg^{-1}) and a pETT11a overexpressed BHMT (18.5 nmol · min^{-1} · mg^{-1}). Total and cytosolic expression levels were similar for wild-type and mutants,

Table 3 Kinetic parameters for BHMT

BHMT activity was measured as described in the Experimental section, for 1 h at 37 °C. Kinetic studies were performed in the 1 μM to 6.5 mM concentration range for both substrates Hcy and betaine. Affinities for the substrates in mutants with less than 15% of the wild-type activity were not determined (n.d.).

	V_{max} (nmol · min^{-1} · mg^{-1})	k_{cat} (s^{-1})	K_m (μM) (Hcy)	K_m (μM) (Betaine)
Wild-type	18.67 ± 0.14	0.014	106.4 ± 11.3	333.3 ± 25.3
E21A	8.39 ± 0.25	0.006	17.47 ± 3.2	138.5 ± 13.2
E21K	12.82 ± 0.34	0.009	72.66 ± 8.9	195.1 ± 16.87
D26A	6.81 ± 0.17	0.0051	62.93 ± 2.6	1174 ± 102.6
D26I	2.86 ± 0.67	0.0021	n.d.	n.d.
T73G	6.09 ± 0.2	0.0045	49.25 ± 7.9	258.4 ± 17.1
F74A	9.69 ± 0.26	0.0072	57.44 ± 7.8	968.6 ± 99.5
Y77A	1.36 ± 0.01	0.001	n.d.	n.d.
A119G	10.05 ± 0.3	0.0075	67.98 ± 9.46	305.6 ± 29.6
E159G	0.305 ± 0.02	0.00023	n.d.	n.d.
E159K	0.11 ± 0.025	0.000082	n.d.	n.d.
T184G	7.77 ± 0.6	0.0058	34.46 ± 13.2	548.1 ± 55.4
C186S	8.01 ± 0.26	0.006	74.45 ± 11.1	206.5 ± 19.9
C186A	10.12 ± 0.41	0.0076	24.73 ± 5.64	185.2 ± 11.4

as judged by Coomassie Blue staining of SDS/PAGE gels (results not shown). The purification yield was similar (approx. 4 mg/g of bacteria), and in addition an anti-BHMT antiserum was able to recognize all the mutants with similar specificity. Moreover, the purification procedure was the same for all of the proteins, suggesting that the BHMT conformation was not significantly altered in the mutants. Far-UV CD spectroscopy showed no significant difference among spectra (Figure 5). The content in main SS elements has been calculated and appears in Table 2. The composition obtained compares favourably with the values from prediction methods and with those derived from the X-ray structure of human BHMT for α-helix content, whereas the β-sheet percentage resulting from this analysis is overestimated. This observation concurs with the difficulties in the accurate assignment of β-sheet structural elements from CD spectra, which are often rigorously resolved using complementary spectroscopies [41,49,50]. In addition, the oligomeric state of the mutants was also evaluated by gel-filtration chromatography. No significant change in the elution pattern was observed, the elution volume corresponding to that of a globular protein with an estimated molecular mass of 187 kDa. Therefore it can be inferred that none of the residues studied plays a significant role in the association of the subunits.

All the mutant proteins exhibited decreased activity (Table 3). Four groups can be identified, those with approx. 70% of wild-type activity [E21K (Glu^{21} → Lys), E21A, C186S, C186A, F74A, A119G, T73G, T184G], those with an intermediate level (D26A), those with 15–10% of activity (Y77A, D26I) and finally those with less than 2% of the original level (E159G, E159K). To get an insight into the significance of these changes, kinetic studies for all the mutants within the first three groups were carried out (Table 3). This type of analysis was not performed for the rest of the mutants due to the low sensitivity of the assay; however, this analysis is accurate for BHMT activity determinations [51]. The K_m values obtained for the recombinant wild-type protein differed from those published previously for the rat liver purified BHMT [52,53], being 9- and 3-fold higher for Hcy and betaine respectively. In fact, the K_m values obtained for Hcy are closer to those published for the human liver purified enzyme [54] than to those for the recombinant human BHMT [13]. Regarding betaine, the K_m values differed markedly from those published for the human liver enzyme, which are approx. 2.3 mM [13]. Mutant

proteins E21A, T73G, F74A, C186A and T184G showed increases in affinity for Hcy. Changes of either sign were also detectable in betaine affinity. Slight increases, approx. 30%, were observed for E21A, E21K, C186S and C186A. In contrast, decreases (> 3-fold) were observed for D26A and F74A, the K_m values reaching the millimolar range as described for human liver BHMT [13]. Thus, based on these results, it can be inferred that Asp[26] and Phe[74] play a role in betaine binding, since the mutants generated for these residues show a diminished activity and a dramatic change in the affinity for this substrate. With respect to Hcy binding, the strongest effect, a 4–5-fold increase in affinity, was shown by E21A and C186A. However, the hydroxide-dependent conversion of Hcy thiolactone into Hcy is not quantitative [55] and, hence, has a clear effect on the real concentration of the amino acid in each assay, which is difficult to estimate. Therefore it could be suggested that Glu[21] and Cys[186] may play a role in Hcy binding, but their importance cannot be directly quantified.

Recently, the structures of human BHMT, Zn^{2+}-depleted and Zn^{2+}-repleted in complex with a transition-state analogue, *S*-(δ-carboxybutyl)-L-homocysteine (CB-Hcy), have been published [8]. The overall fold described for the monomer is an $(\alpha,\beta)_8$ barrel, as proposed in our structural model. Moreover, the complex with CB-Hcy highlighted the role of some amino acids in the active site, among them Asp[26], Glu[159] and Tyr[77] (numbered according to the human BHMT sequence). These are the residues that show important effects on activity in our mutagenesis study (Table 3). The postulated roles for these residues are related to Hcy binding (Asp[26]), establishing stereospecificity for L-Hcy (Glu[159]), and interacting with the carboxy group of the methyl donor (Tyr[77]) [8]. Activity measurements of the corresponding mutants revealed strong reductions in methionine synthesis in all the cases, except for D26A, for which a substantial decrease in affinity for betaine was detectable, an effect also shown by F74A. Substitutions performed involving Asp[26] are related to changes in the charge and the volume of the side chain (a slight decrease in D26A and an increase in D26I). It is relevant to note that D26A affects the affinity for betaine, in contrast with the role of Asp[26] in Hcy binding proposed and deduced from its high level of conservation among the thiol/selenol methyltransferase family [8]. In the human BHMT crystal structure, Asp[26] interacts with the backbone amide of Gln[72] from β2-strand. This interaction brings apart the β1- and β2-strands, creating a cleft between them, which has been proposed to be important in Hcy accommodation. Nevertheless, our results suggest another role for Asp[26] related to betaine binding. Accordingly, Asp[26] seems to be involved in shaping the active site, and this role could also be reflected by changes in activity and the affinity for betaine. An increase in the K_m value for betaine was also noticed with F74A, where a reduction in the length and volume of the side chain is produced, thus indicating a role for the aromatic ring in betaine binding. Phe[74] precedes Phe[76] and Tyr[77], which are involved in betaine binding, as suggested in the CB-Hcy complex with human BHMT. In addition, Phe[74] is packed against other non-polar residues, and substitution of phenylalanine by alanine would break this packing, resulting in a disruption of the local conformation, and therefore affecting betaine binding.

The results obtained with Glu[159] mutants confirmed the crucial role of its side chain in BHMT activity, since either of the substitutions performed (elimination of the side chain or change of charge in the ϵ group) abolished methionine production. Moreover, the carboxybutyl moiety of CB-Hcy served to suggest the binding site for glycinebetaine through its carboxy group, a role ascribed to Tyr[77] of human BHMT [8]. Again, our model suggested an essential role for this residue, and in fact its substitution by alanine produced a marked decrease in activity, thus highlighting the importance of its side chain.

Other residues located close to the Hcy-binding site also show interesting features when their substitution is carried out. A conservative change performed on Cys[186], such as that produced by the inclusion of serine, exerted no effect on substrate affinity. However, in C186A, when the amino acid chain is shortened and the -SH or -OH groups disappear, an increase in affinity for Hcy is detectable, suggesting a role for this residue in substrate binding. Such a role could not be ascribed in the human crystal structure, since this is one of the five cysteine residues, considered non-essential, that were mutated to avoid aggregation [8]. In addition, mutation of Thr[184], just two residues downstream in the sequence, also affected Hcy affinity. Thr[184] interacts through its side chain with Asn[216], which in motif I (GVNC) is involved in Zn^{2+} binding. Elimination of the side chain by substitution with glycine suppressed this interaction and, hence, it could have an indirect effect on ion binding and therefore on Hcy affinity. Mutations performed on human Asn[216] showed a decrease in activity, which in the case of N216A was comparable with that produced by T184G, but effects on affinity were not explored [14].

Finally, all our results indicate that the structural model presented here shows the main features of the BHMT monomer and allows the identification of key residues for enzyme activity. Their importance has been confirmed by site-directed mutagenesis and kinetic studies, defining a further role for Asp[26] in the active site. The results obtained are consistent with those derived from X-ray diffraction, thus suggesting that these types of structural models can be useful tools for other families of enzymes with unknown structure, allowing the identification of key residues involved in catalysis.

We thank Professor T. L. Blundell for his valuable suggestions, A. Cerqueira for technical assistance and Dr D. Laurents and B. Ashley Morris for style and grammatical corrections. This work was supported by the Fondo de Investigación Sanitaria (grant no. 01/1077 to M.A.P.) and the Ministerio de Ciencia y Tecnología (grant no. BIO2000-1664 to M.G. and BIO2000-1279 to J.S.-A.).

REFERENCES

1 Mato, J. M., Alvarez, L., Ortiz, P. and Pajares, M. A. (1997) *S*-adenosylmethionine synthesis: molecular mechanisms and clinical implications. Pharmacol. Ther. **73**, 265–280
2 Cantoni, G. L. (1975) Biochemical methylations: selected aspects. Annu. Rev. Biochem. **44**, 435–441
3 Finkelstein, J. D. and Mudd, S. H. (1967) *Trans*-sulfuration in mammals. The methionine-sparing effect of cystine. J. Biol. Chem. **242**, 873–880
4 Motulski, A. G. (1996) Nutritional ecogenetics: homocysteine-related arteriosclerotic vascular disease, neural tube defects, and folic acid. Am. J. Hum. Genet. **58**, 17–20
5 Refsum, H., Ueland, P. M., Nygard, O. and Vollset, S. E. (1998) Homocysteine and cardiovascular disease. Annu. Rev. Med. **49**, 31–62
6 Bose, N. and Momany, C. (2001) Crystallization and preliminary X-ray crystallographic studies of recombinant human betaine-homocysteine *S*-methyltransferase. Acta Crystallogr. **D57**, 431–433
7 González, B., Pajares, M. A., Too, H.-P., Garrido, F., Blundell, T. L. and Sanz-Aparicio, J. (2002) Crystallisation and preliminary X-ray study of recombinant betaine-homocysteine *S*-methyltransferase from rat liver. Acta Crystallogr. **D58**, 1507–1510
8 Evans, J. C., Huddler, D. P., Jiracek, J., Castro, C., Millian, N. S., Garrow, T. A. and Ludwig, M. L. (2002) Betaine-homocysteine methyltransferase; zinc in a distorted barrel. Structure **10**, 1159–1171
9 Sunden, S. L., Renduchintala, M. S., Park, E. I., Miklasz, S. D. and Garrow, T. A. (1997) Betaine-homocysteine methyltransferase expression in porcine and human tissues and chromosomal localization of the human gene. Arch. Biochem. Biophys. **345**, 171–174
10 Delgado-Reyes, C. V., Wallig, M. A. and Garrow, T. A. (2001) Immunohistochemical detection of betaine-homocysteine *S*-methyltransferase in human, pig, and rat liver and kidney. Arch. Biochem. Biophys. **393**, 184–186

11 Rao, P. V., Garrow, T. A., John, F., Garland, D., Millian, N. S. and Zigler, Jr, J. S. (1998) Betaine-homocysteine methyltransferase is a developmentally regulated enzyme crystallin in rhesus monkey lens. J. Biol. Chem. **273**, 30669–30674

12 Sowden, M. P., Collins, H. L., Smith, H. C., Garrow, T. A., Sparks, J. D. and Sparks, C. E. (1999) Apolipoprotein B mRNA and lipoprotein secretion are increased in McArdle RH-7777 cells by expression of betaine-homocysteine *S*-methyltransferase. Biochem. J. **341**, 639–645

13 Millian, N. S. and Garrow, T. A. (1998) Human betaine-homocysteine methyltransferase is a zinc metalloenzyme. Arch. Biochem. Biophys. **356**, 93–98

14 Breksa, III, A. P. and Garrow, T. A. (1999) Recombinant human liver betaine-homocysteine *S*-methyltransferase: identification of three cysteine residues critical for zinc binding. Biochemistry **38**, 13991–13998

15 Heil, S. G., Lievers, K. J., Boers, G. H., Verhoef, P., den Heijer, M., Trijbels, F. J. and Blom, H. J. (2000) Betaine-homocysteine methyltransferase (BHMT): genomic sequencing and relevance to hyperhomocysteinemia and vascular disease in humans. Mol. Genet. Metab. **71**, 511–519

16 Finkelstein, J. D. and Martin, J. J. (1986) Methionine metabolism in mammals. Adaptation to methionine excess. J. Biol. Chem. **261**, 1582–1587

17 Finkelstein, J. D., Harris, B. J., Martin, J. J. and Kyle, W. E. (1982) Regulation of hepatic betaine-homocysteine methyltransferase by dietary methionine. Biochem. Biophys. Res. Commun. **108**, 344–348

18 Williams, Jr, J. N., Monson, W. J., Sreenivasan, A., Dietrich, L. S., Harper, A. E. and Elvehjem, C. A. (1953) Effects of a vitamin B_{12} deficiency on liver enzymes in the rat. J. Biol. Chem. **202**, 151–156

19 Finkelstein, J. D., Cello, J. P. and Kyle, W. E. (1974) Ethanol-induced changes in methionine metabolism in rat liver. Biochem. Biophys. Res. Commun. **61**, 525–531

20 Klee, W. A., Richards, H. H. and Cantoni, G. L. (1961) The synthesis of methionine by enzymic transmethylation. Biochim. Biophys. Acta **54**, 157–164

21 Forestier, M., Reichen, J. and Solioz, M. (1996) Application of mRNA differential display to liver cirrhosis: reduced fetuin expression in biliary cirrhosis in the rat. Biochem. Biophys. Res. Commun. **225**, 377–383

22 Avila, M. A., Berasain, C., Torres, L., Martin-Duce, A., Corrales, F. J., Yang, H., Prieto, J., Lu, S. C., Caballeria, J., Rodes, J. et al. (2000) Reduced mRNA abundance of the main enzymes involved in methionine metabolism in human liver cirrhosis and hepatocellular carcinoma. J. Hepatol. **33**, 907–914

23 Park, E. I., Renduchintala, M. S. and Garrow, T. A. (1997) Diet-induced changes in hepatic betaine-homocysteine methyltransferase activity are mediated by changes in the steady-state level of its mRNA. J. Nutr. Biochem. **8**, 541–545

24 Sandu, C., Nick, P., Hess, D., Schiltz, E., Garrow, T. A. and Brandsch, R. (2000) Association of betaine-homocysteine *S*-methyltransferase with microtubules. Biol. Chem. **381**, 619–622

25 Coelho-Sampaio, T., Ferreira, S. T., Castro, Jr, E. J. and Vieyra, A. (1994) Betaine counteracts urea-induced conformational changes and uncoupling of the human erythrocyte Ca^{2+} pump. Eur. J. Biochem. **221**, 1103–1110

26 Altschul, S. F., Madden, T. L., Schaffer, A. A., Zhang, J., Zhang, Z., Miller, W. and Lipman, D. J. (1997) Gapped BLAST and PSI-BLAST: a new generation of protein database search programs. Nucleic Acids Res. **25**, 3389–3402

27 Thompson, J. D., Higgins, D. G. and Gibson, T. J. (1994) CLUSTAL W: improving the sensitivity of progressive multiple sequence alignment through sequence weighting, position-specific gap penalties and weight matrix choice. Nucleic Acids Res. **22**, 4673–4680

28 Rost, B. (1996) PHD: predicting one-dimensional protein structure by profile based neural networks. Methods Enzymol. **266**, 525–539

29 McGuffin, L. J., Bryson, K. and Jones, D. T. (2000) The PSIPRED protein structure prediction server. Bioinformatics **16**, 404–405

30 Cuff, J. A., Clamp, M. E., Siddiqui, A. S., Finlay, M. and Barton, G. J. (1998) JPred: a consensus secondary structure prediction server. Bioinformatics **14**, 892–893

31 Fischer, D., Barret, C., Bryson, K., Elofsson, A., Godzik, A., Jones, D., Karplus, K. J., Kelley, L. A., MacCallum, R. M., Pawowski, K. et al. (1999) CAFASP-1: critical assessment of fully automated structure prediction methods. Proteins: Struct. Function Genet. **S3**, 209–217

32 Jones, D. T., Taylor, W. R. and Thornton, J. M. (1992) A new approach to protein fold recognition. Nature (London) **358**, 86–89

33 Fischer, D. (2000) Hybrid fold recognition: combining sequence derived properties with evolutionary information, Pac. Symp. Biocomput. 2000, 119–130

34 Sali, A. and Blundell, T. L. (1993) Comparative modelling by satisfaction of spatial restraints. J. Mol. Biol. **234**, 779–815

35 Wang, Z. and Quiocho, F. A. (1998) Complexes of adenosine deaminase with two potent inhibitors: X-ray structures in four independent molecules at pH of maximum activity. Protein Sci. **37**, 8314–8324

36 Luthy, R., Bowie, J. V. and Eisenberg, D. (1992) Assessment of protein models with three-dimensional profiles. Nature (London) **356**, 83–85

37 Laskowski, R. A., MacArthur, M. W., Moss, D. S. and Thornton, J. M. (1993) PROCHECK: a program to check the stereochemical quality of protein structures. J. Appl. Crystallogr. **26**, 283–291

38 Mizuguchi, K., Deane, C. M., Blundell, T. L., Johnson, M. S. and Overington, J. P. (1998) JOY: protein sequence structure representation and analysis. Bioinformatics **14**, 617–623

39 Sali, A. and Blundell, T. L. (1990) Definition of general topological equivalence in protein structures. A procedure involving comparison of properties and relationships thought simulated annealing and dynamic programming. J. Mol. Biol. **212**, 403–428

40 Sanger, F., Nicklen, S. and Coulson, A. R. (1977) DNA sequencing with chain-terminating inhibitors. Proc. Natl. Acad. Sci. U.S.A. **74**, 5463–5467

41 Medrano, F. J., Gasset, M., López-Zumel, C., Usobiaga, P., García, J. L. and Menéndez, M. (1996) Structural characterization of the unligated and choline-bound forms of the major pneumococcal autolysin LytA amidase: conformational transitions induced by temperature. J. Biol. Chem. **271**, 29152–29161

42 Mingorance, J., Alvarez, L., Sánchez-Góngora, E., Mato, J. M. and Pajares, M. A. (1996) Site-directed mutagenesis of rat liver *S*-adenosylmethionine synthetase. Identification of a cysteine residue critical for the oligomeric state. Biochem. J. **315**, 761–766

43 Drennan, C. L., Huang, S., Drummond, J. T., Matthews, R. G. and Ludwig, L. (1994) How a protein binds B_{12}: a 3.0 Å X-ray structure of B_{12}-binding domains of methionine synthase. Science **266**, 1669–1674

44 Dixon, M. M., Huang, S., Matthews, R. G. and Ludwig, L. (1996) The structure of the C-terminal domain of methionine synthase: *S*-adenosylmethionine for reductive methylation. Structure **4**, 1263–1275

45 Finkelstein, J. D. and Martin, J. J. (1984) Methionine metabolism in mammals. Distribution of homocysteine between competing pathways. J. Biol. Chem. **259**, 9508–9513

46 Wilson, L. A. and Quiocho, F. A. (1993) A pre-transition-state mimic of an enzyme: X-ray structure of adenosine deaminase with bound 1-deazaadenosine and zinc-activated water. Biochemistry **32**, 1689–1694

47 Wilson, D. K., Rudolph, F. B. and Quiocho, F. A. (1991) Atomic structure of adenosine deaminase complexed with a transition-state analog: understanding catalysis and immunodeficiency mutations. Science **252**, 1278–1284

48 Trikha, J., Theil, E. C. and Allewell, N. M. (1995) High resolution crystal structures of amphibian red-cell L ferritin: potential roles for structural plasticity and solvation in function. J. Mol. Biol. **248**, 949–967

49 Gasset, M., Saiz, J. L., Laynez, J., Sanz, L., Gentzel, M., Topper-Petersen, E. and Calvete, J. J. (1997) Conformational features and thermal stability of bovine seminal plasma protein PDC-109 oligomers and phosphorylcholine-bound complexes. Eur. J. Biochem. **250**, 735–744

50 Goormaghtigh, E., Cabiaux, V. and Ruysschaert, J. M. (1994) Determination of soluble and membrane protein structure by Fourier transform infrared spectroscopy. III. Secondary structures. Subcell. Biochem. **23**, 405–450

51 Mulligan, J. D., Laurie, T. J. and Garrow, T. A. (1998) An assay for betaine-homocysteine methyltransferase activity based on the microbiological detection of methionine. J. Nutr. Biochem. **9**, 351–354

52 Finkelstein, J. D., Harris, B. J. and Kyle, W. E. (1972) Methionine metabolism in mammals: kinetic study of betaine-homocysteine methyltransferase. Arch. Biochem. Biophys. **153**, 320–324

53 Lee, K. H., Cava, M., Amiri, P., Ottoboni, T. and Lindquist, R. N. (1992) Betaine: homocysteine methyltransferase from rat liver: purification and inhibition by a boronic acid substrate analog. Arch. Biochem. Biophys. **292**, 77–86

54 Skiba, W. E., Wells, M. S., Mangum, J. H. and Awad, W. M. (1987) Betaine-homocysteine *S*-methyltransferase (human). Methods Enzymol. **143**, 384–388

55 Duerre, J. A. and Miller, C. H. (1966) Metabolism of *S*-adenosyl-L-homocysteine *in vivo* by the rat. Anal. Biochem. **17**, 310–315

Received 27 September 2002/9 December 2002; accepted 17 December 2002
Published as BJ Immediate Publication 17 December 2002, DOI 10.1042/BJ20021510